

## REVIEW ARTICLE

Toward functional bone bioprinting:  
Addressing the overlooked challenges of  
mechanical compliance**Amin Ebrahimi Sadrabadi<sup>1,2</sup>**, **Payam Baei<sup>3</sup>**, **Yalda Alibeigian<sup>1</sup>**,  
**Mohamadreza Baghaban Eslaminejad<sup>1\*</sup>**, and **Samaneh Hosseini<sup>1,3\*</sup>**<sup>1</sup> Department of Stem Cells and Developmental Biology, Cell Science Research Center, Royan Institute for Stem Cell Biology and Technology, ACECR, Tehran, Iran<sup>2</sup> Department of Tissue Engineering, Faculty of Basic Sciences and Advanced Technologies in Medicine, Royan Institute, ACECR, Tehran, Iran<sup>3</sup> Department of Cell Engineering, Cell Science Research Center, Royan Institute for Stem Cell Biology and Technology, ACECR, Tehran, Iran

(This article belongs to the *Special Issue: Biofabrication Breakthroughs: Innovation and Application in Bioprinting, Biomaterials, and Organoid*)

**Abstract**

Three-dimensional bioprinting has emerged as a transformative biofabrication technology capable of engineering complex tissue constructs for regenerative medicine. While considerable progress has been made in replicating soft tissues using hydrogel-based bioprinting, the fabrication of mechanically robust bone-mimicking constructs remains a significant challenge. The mechanical heterogeneity of bone, including its anisotropic structure, varying mineral density, and intricate extracellular matrix composition, complicates the development of bioinks that can simultaneously achieve printability, structural integrity, and cellular viability. Recent advancements have focused on optimizing the mechanical properties of bioinks through composite hydrogels, osteoinductive nanomaterials, and bioactive moieties that enhance cell adhesion and differentiation. This review examines the role of mechanical cues in directing mesenchymal stem cell fate, the interplay between material stiffness and osteogenesis, and strategies to enhance bioink performance. We highlight limitations in mechanical compliance and propose novel biomaterial designs, crosslinking strategies, and scaffold functionalization to overcome these barriers. This review aims to bridge the gap between biomaterials science and clinical translation, with the ultimate goal of advancing functional bone graft substitutes.

**Keywords:** 3D bioprinting; Bioinks; Bone tissue engineering; Extracellular matrix; Mechanical compliance; Regenerative medicine

**\*Corresponding authors:**Mohamadreza Baghaban  
Eslaminejad  
(eslami@royaninstitute.org)Samaneh Hosseini  
(hosseini.samaneh@royaninstitute.  
org)

**Citation:** Sadrabadi AE, Baei P, Alibeigian Y, Eslaminejad MB, Hosseini S. Toward functional bone bioprinting: Addressing the overlooked challenges of mechanical compliance.

*Int J Bioprint.* 2026;12(1):19-37.  
doi: 10.36922/IJB025420425

**Received:** October 15, 2025

**Revised:** November 26, 2025

**Accepted:** December 3, 2025

**Published online:** December 3, 2025

**Copyright:** © 2025 Author(s). This is an Open Access article distributed under the terms of the Creative Commons Attribution License, permitting distribution, and reproduction in any medium, provided the original work is properly cited.

**Publisher's Note:** AccScience Publishing remains neutral with regard to jurisdictional claims in published maps and institutional affiliations.

**1. Introduction**

Three-dimensional (3D) bioprinting is an impressive technology for artificial bone production compared to other engineering approaches. This technology seeks to biofabricate a scaffold in a 3D architecture and mimics the exact positioning of various cell types under controlled 3D gradients of growth factors or biological molecules. As the first ingredient in the process of 3D bioprinting, bioinks need to be adjusted

by combination with growth factors, cells, and different materials, making it a challenging process. Regardless of the precise management of the nano- to macro-scale transformations in the engineered bioinks, it still encounters some difficulties that alter the final constructs and are not thoroughly investigated yet. Achieving mechanical compliance in bioprinted constructs that closely mimic native bone tissue remains a significant challenge in tissue engineering.

Recent advancements have focused on developing composite hydrogels and hybrid scaffolds that integrate multiple materials to replicate the complex mechanical properties of bone. For instance, combining natural polymers like gelatin methacrylate (GelMA) with inorganic components such as hydroxyapatite has shown promise in enhancing the mechanical strength and bioactivity of bioprinted scaffolds. These composite materials not only provide the necessary structural integrity but also support cellular functions, promoting tissue regeneration.<sup>1,2</sup> However, optimizing the composition and fabrication techniques to achieve the desired mechanical properties while maintaining biocompatibility requires further research. Understanding the interplay between material properties and cellular responses is crucial for the successful application of these advanced biomaterials in clinical settings.

Functional biofabrication has been hindered by various biological and nonbiological challenges that include the lack of control over cell shape, size, and orientation, inability to create complex cellular structures, and the difficulty of fabricating and controlling the mechanical properties of the microenvironments surrounding the cells *in vivo*. The mechanical properties of the extracellular matrix (ECM), particularly its stiffness, play a pivotal role in directing the fate of mesenchymal stem cells (MSCs). Studies have demonstrated that MSCs cultured on substrates with stiffness analogous to that of bone tissue (~40 kPa) tend to undergo osteogenic differentiation, whereas those on softer substrates resembling brain tissue (~0.1–1 kPa) are inclined toward neurogenic pathways. Intermediate stiffness levels, similar to muscle tissue (~10 kPa), have been shown to promote myogenic differentiation.<sup>3</sup> This mechanotransduction involves the regulation of gene expression and cellular functions, such as proliferation and migration, mediated through pathways like RhoA/ROCK.<sup>4</sup> Understanding these dynamics is crucial for developing bioinks in 3D bioprinting that not only provide structural integrity but also mimic native tissue stiffness to guide desired cellular behaviors.

Many attempts have been made to optimize the mechanical features of bioink. Utilization of composite

hydrogels and additive compounds, such as osteo-promotive materials and active moieties, has transformed hydrogels into advanced materials with improved mechanical characteristics.<sup>5-7</sup> It was found that silver and platinum alloy nanoparticles, as well as zinc ions, improve the biological and mechanical performance of bioink and matrix deposition of MSCs.<sup>8</sup> The thiol-ene or click chemistry makes active moieties an appropriate agent to regulate biological and nonbiological properties of biomaterials.<sup>9</sup> Thiol-ene click chemistry is a robust and efficient reaction between thiol groups and carbon-carbon double bonds (alkenes), typically initiated by light or radical initiators. This reaction proceeds rapidly under mild conditions, making it highly suitable for biomedical applications. One of the key advantages of thiol-ene chemistry is its high specificity and yield, allowing for the precise fabrication of hydrogels with controllable crosslinking densities.<sup>10</sup> This precision enables tuning mechanical properties to match those of native tissues, crucial in tissue engineering and regenerative medicine. Additionally, the reaction's insensitivity to oxygen and its cytocompatibility make it ideal for *in situ* gelation, facilitating the encapsulation of cells and bioactive molecules without compromising their viability or function. Recent studies have demonstrated the successful application of thiol-ene click hydrogels in controlled therapeutic delivery and tissue scaffolding, highlighting their potential in advancing bioprinting technologies.<sup>11</sup> Additionally, the Janus-faced hydrogen bonding moieties coupled to the supramolecular network provide excellent network stability and improved mechanical strength.<sup>12</sup> As a result, hydrogen bonds are more stable due to the presence of active moieties, giving rise to stronger network structures. In addition, thiol-ene click chemistry produces a more efficient and cost-effective way of creating and regulating these moieties, allowing for greater control over the mechanical properties of the bioink.

Superior biofabrication approaches can develop biocompatible and shear-thinning bioinks, which could mimic bone mechanical strength while simultaneously maintaining cell/stem cell viability. Shear-thinning and thixotropic properties have hindered the development of novel mechanically optimized bioinks. These properties describe the nonlinear relationship between shear stress, shear strain, and the time-dependent changes in the viscosity of a fluid after applying force. Additives that are added to bioink to improve its mechanical features can interfere with bioink printability and counteract these features. Viscose biomaterials, such as chitosan and alginate, as well as nanoscale biomaterials, such as clay and hydroxyapatite, increase viscosity excessively, and disrupt printability.<sup>13,14</sup> Therefore, in order to ensure

the printability of bioink, it is important to choose additives carefully and in moderation. For bioprinted bone constructs to successfully integrate and remodel into functional bone tissue, it is imperative that they recapitulate this mechanical environment. Failure to provide an appropriate mechanical environment have significant consequences.<sup>15</sup> Scaffolds that are too stiff may lead to stress shielding, where the implant carries a disproportionate amount of the load, preventing the surrounding native bone and the cells within the construct from experiencing the mechanical stimuli necessary for growth and remodeling. This can result in bone resorption and implant loosening.<sup>16</sup> Conversely, scaffolds that are too weak will fail to provide the necessary support for cell proliferation and differentiation and may collapse under physiological loading. Therefore, the ideal bioprinted bone construct should possess mechanical properties that are not only compatible with the target anatomical location but also tailored to promote a specific cellular response.<sup>17</sup> This concept of “mechano-mimicking” is a central theme in modern bone tissue engineering, and a key focus of this review.

This review explores the complexities of bone bioprinting, focusing on the mechanical challenges in replicating native bone structures. We discuss the factors influencing bone mechanical strength, the influencing factors of printability, the distinct requirements for different bone bioprinting applications, and the potential strategies to overcome current limitations in bioink design (Figure 1).

## 2. Factors affecting mechanical properties of bone constructs

### 2.1. Complexity and mechanical strength of bone

Bones, as connective tissues, provide a rigid framework to support soft organs and help balance minerals, such as calcium and phosphate.<sup>18</sup> As a highly dynamic organ, a bone undergoes the process of remodeling that supports the minerals' hemostasis and participates in preserving the integrity of the skeleton through self-renewal.<sup>19-21</sup> Cortical and trabecular bones have been shown to perform these functions accurately. The bone strength, mineral density (BMD), and porosity of cortical and trabecular bone are substantially different.<sup>22</sup> These features are distinct in age, gender, and ethnicity.<sup>23</sup> Specifically, BMD is lower in women than men, decreasing almost linearly with age.<sup>24,25</sup> As measured by finite element analysis (FEA), young women have softer bones than young men, and both genders lose bone strength with aging.<sup>26,27</sup> The bone complexity has also extended to the microarchitecture of the different bone tissues. Trabecular microarchitecture and conformation vary by ethnicity and gender.<sup>28</sup> This variety consists

of different ratios of plate-like and rod-like trabeculae morphology, making bone tissue a heterogeneous organ in terms of mechanical strengths (Figure 2A). The difference between the structures of these two types of bones has caused the variation in their mechanical strengths; as the compressive strength of the trabecular bone is estimated to fall in the range of 2–12 MPa with the elastic modulus of 0.1–5 GPa, while this value raises to 100–150 MPa for cortical bone with elastic modulus ranging from 7 to 20 GPa.<sup>29,30</sup> These properties vary between different types of bones as the needed force to break down the femur is around 74131.83 N, which decreases to 5833.99 N, 4412.99 N, and 1882.88 N for the humerus, tibia and patella, respectively.<sup>31</sup> This mechanical and microstructural diversity has raised a desire for a method that provides precise structural control in three dimensions.

### 2.2. Heterogeneity of bone structure and composition

A bone is a mineralized tissue that is a mixture of collagen and noncollagenous proteins, water, minerals, and some organics, whose mechanical strength can be determined based on various factors.<sup>32</sup> These factors include the type of bone (primary, woven, or both), density, the arrangement of collagen fibers, the amount and type of noncollagenous proteins, and the quantity of minerals and water present in the bone. All of these components work together to provide a bone with its unique strength and flexibility. Each bone is characterized by a randomized distribution of cells, collagen fibers, and osteoids.<sup>33,34</sup> Since lamellar bones participate in fracture repair and embryonic development, they show more rigidity compared to primary bones in the adult skeleton.<sup>33</sup> Cortical bone possesses greater density and resistance to stress, while trabecular bone, with its honeycomb-like structure, is the opposite. Trabecular bone's elasticity increases and its stress resistance decreases to 50 MPa,<sup>35,36</sup> thereby increasing elasticity and decreasing stress resistance. This is because a lamellar bone has a larger quantity of collagen fibers with higher tensile strength than a primary bone. The increased stiffness of lamellar bones is attributed to their greater mineral content, which increases their density and strength. Cortical bone has a greater ratio of mineral to organic matter, which increases its density and resistance to stress. Trabecular bone has a porous structure and a much lower mineral to organic matter ratio, which reduces its density and strength, but increases its elasticity and decreases its stress resistance.<sup>37</sup> The degree and quality of mineralization is another factor that could change related mechanical properties, such as elasticity, plasticity, and viscoelasticity, as low mineralization can lead to the fragility of bones.<sup>38,39</sup> Several studies have delineated that the mineralization pattern of bone plates and their

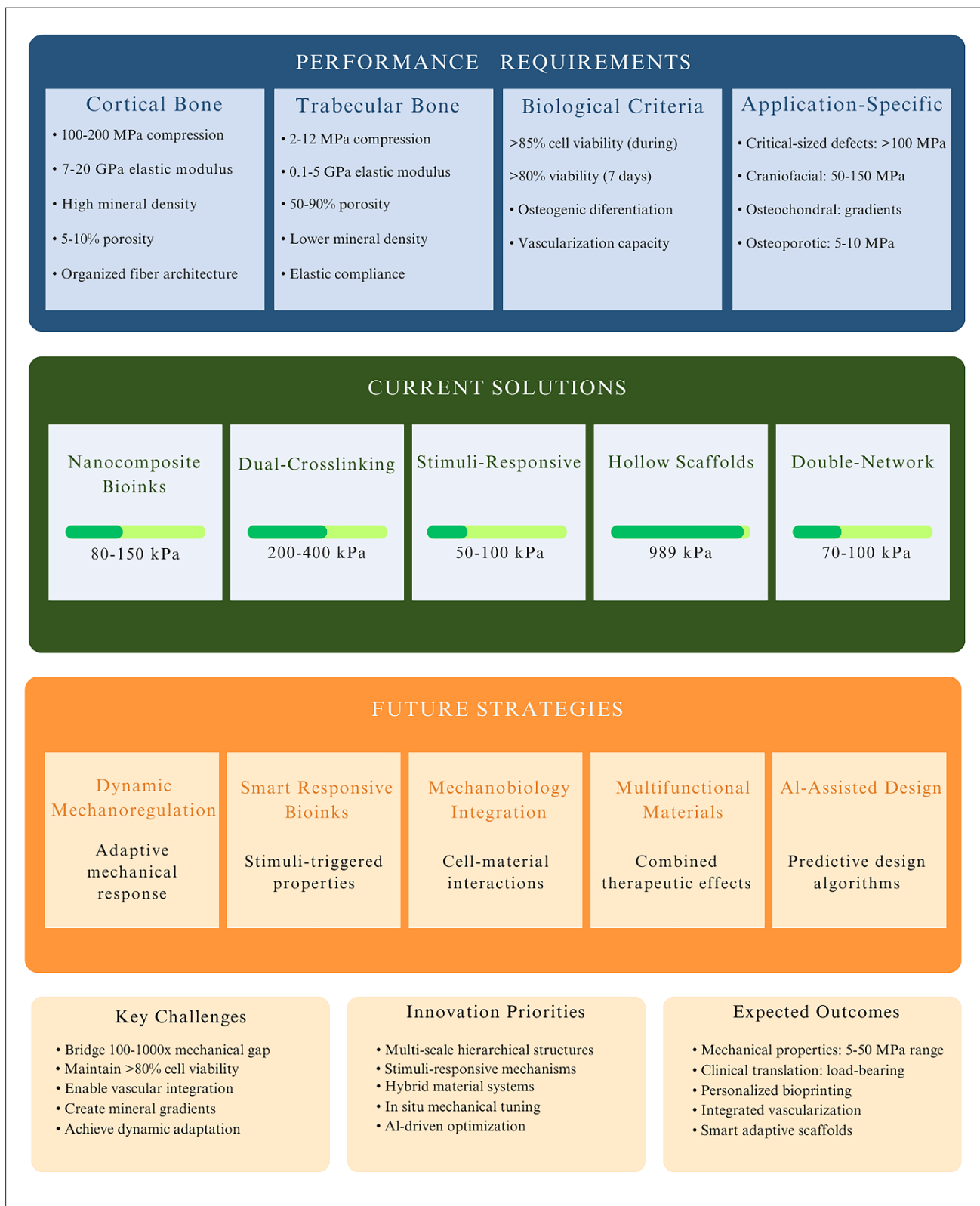


**Figure 1.** Comprehensive framework for mechanical compliance in bone bioprinting. Top panel presents performance requirements across bone types and clinical applications. Middle panel maps current technological solutions achieving bone mechanical properties. Bottom panel outlines future innovation strategies. Bottom boxes highlight key challenges, innovation priorities, and expected outcomes.

absolute degree of mineralization could determine the mechanical strength.<sup>40</sup> This is because mineralization is important for the deposition of collagen and other proteins, which are necessary for the strength of the bone. As mineralization increases, the collagen is better organized and the bones become stronger. This strength is further enhanced by the formation of hydroxyapatite crystals and other minerals, which add to the overall mineralization of the bones. The other contributing factor is porosity, defined by the distribution and magnitude of pores in bones.<sup>41,42</sup> Trabecular and cortical bones are recognized with a porosity varying from 50% to 90% and 5% to 10%, respectively. A slight change in the porosity significantly affects the stiffness and tolerability of the bones,<sup>43,44</sup> because it affects the ability of the bone to absorb energy, the rate of diffusion of substances through the bone, and the strength of the bone. The interaction and a perfect combination of these factors determine the mechanical properties of bones and make the mechanical strength of bones vary from 12.56 to 16.87 kg/mm<sup>2</sup>.<sup>32</sup> Therefore, it is important to understand the correlation between porosity and the mechanical properties of bones, in order to achieve the desired strength and durability

(Figure 2B). Thus far, these unique physical properties of bones have not been mimicked by any of the developed scaffolds and these features have never been successfully replicated with the use of any bioink technology. To this end, further research is needed to accurately replicate the structural composition of bones in order to effectively replicate its mechanical properties in tissue engineering scaffolds and bioinks.

**2.3. Influence of substrate cues**

For a long time, biochemical factors and signals were believed to be the only compounds that affected cell differentiation and determined cellular fate. However, some research has demonstrated that biophysical forces and mechanical stress derived from rigidity, elasticity, and stiffness can also effectively alter proliferation rate, survival, and differentiation and determine cellular fate (Figure 2C).<sup>45,46</sup> In other words, once mechanical forces have been sensed by the cells, during a mechanotransduction process, a cascade of molecular changes and biochemical signals regulate the response of the cells to the physical stimuli.<sup>47</sup> Biophysical stimuli are caused by factors such as surface geometry, fluid shear stress, stain, rigidity,

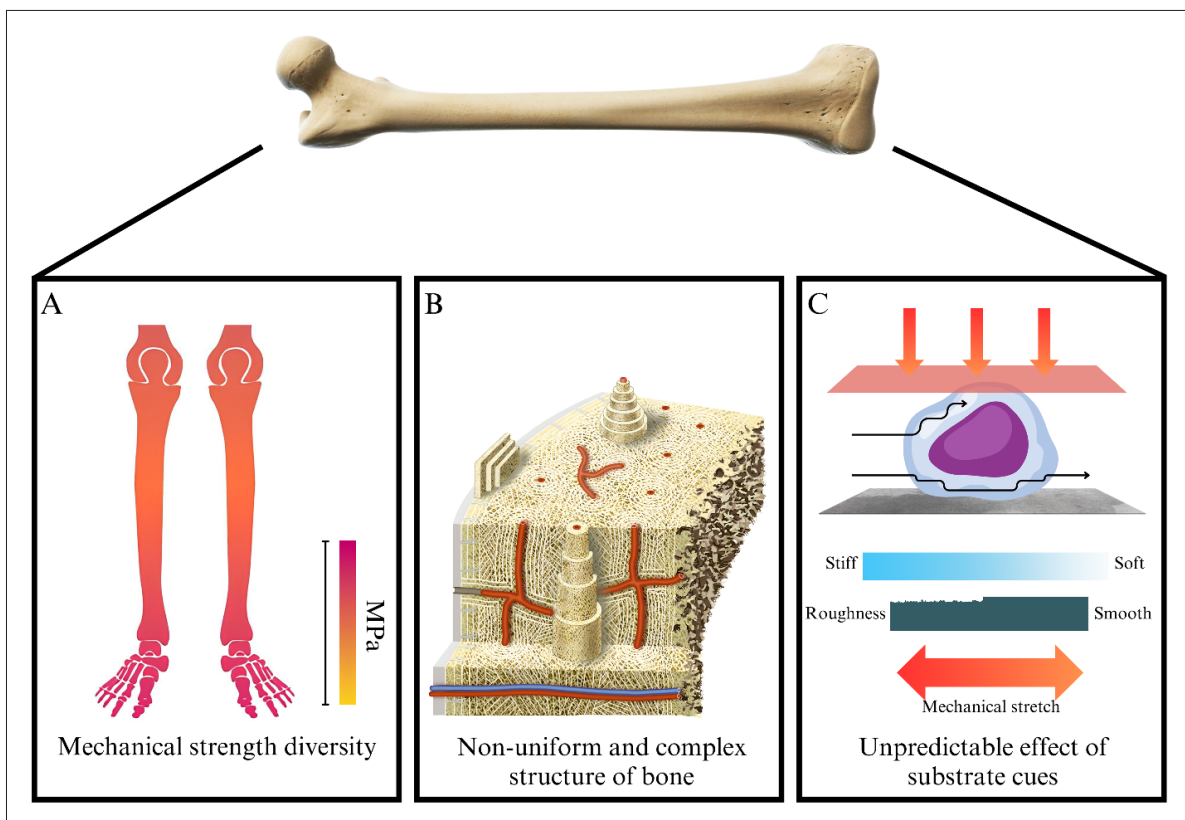


**Figure 2.** Key barriers for developing mechanically optimized bone mimicking constructs. (A) Diversity in bone mechanical strength; (B) Inhomogeneous and complex structure of bones; (C) Heterogeneity and complexity of substrate cues.

stiffness, and matrix surface topography.<sup>48</sup> The influence of physical changes typically begins with the detection of integrins. This eventually results in alteration of cytoskeleton structure by polymerization or contraction and downstream signaling reaching the nucleus.<sup>49</sup> These changes in cytoskeleton structure and downstream signaling can further lead to changes in gene expression, which can alter the cell's phenotypic response, such as cell shape and motility. In a study, it was shown that MSCs differentiate into neurogenic, chondrogenic, or osteogenic lineages when exposed to a range of materials with varying characteristics, from soft to rigid.<sup>50</sup> Controlling these substrate cues in the desired bioink is obviously not straightforward. Thus, understanding how to control the substrate cues to alter gene expression and drive differentiation is a critical step toward achieving directed differentiation of MSCs in bioinks.

A topological property of substrates may affect the self-renewal properties of stem cells, as murine embryonic stem cells (mESCs) cultured on stiff substances kept expressing Nanog and Oct3/4, as well as preserving self-renewal properties.<sup>51</sup> Furthermore, the expression of Sox2, another stemness-related marker, was also higher on stiff substrates compared to soft ones. This finding indicates a potential role for mechanical forces in stem cell differentiation. However, it is important to note that culturing human mesenchymal stem cells (hMSCs) in a 3D hydrogel that has a stiffness over 1 kPa might have a counterproductive effect, since their proliferation has been shown to decrease.<sup>52</sup> This suggests that there is an optimal stiffness that can be used to achieve the desired cell differentiation while still allowing cells to proliferate and function normally. Thus, the ideal mechanical environment should be tailored to the specific cell type in order to maximize their differentiation potential while still allowing them to proliferate and function.

Nevertheless, in another study, hydrogels with low stiffness and quasihexagonally arranged nanopatterns stimulated mechanotransduction, which led to osteogenic differentiation of MSCs.<sup>53</sup> It was also shown that the mechanotransduction of the nanopatterned hydrogels containing RGD (Arg-Gly-Asp) peptide was able to induce the differentiation of MSCs into osteogenic lineages. These results illustrate that cellular responses to substrate cues are not explicit. It is clear that substrate cues have unpredictable effects on stem cells, which makes it challenging to mimic an ideal bioink. The substrate cues can interact with the cells in complex ways and can trigger a cascade of events that lead to different cell responses.<sup>54</sup> This poses a challenge to predict cell response to a given substrate, making it much difficult

to create an ideal bioink that will accurately provoke the desired response.

### 3. Factors affecting the printability of hydrogels

Printability is the main requirement of the bioprinting process, which refers to the capability of a substance, under specific circumstances of bioprinting, to form a 3D object in a layer-by-layer manner.<sup>55</sup> It could be challenging to control the properties of the hydrogel like surface tension, rheological cues, gelation kinetics, swelling properties, and finally the bioprinting process itself.<sup>56</sup> This is because each of these properties affects the printability of the hydrogel, and the ability to form a 3D object depends on the balance between them (Table 1). Additionally, the bioprinting technique itself can be difficult to control, as it requires precise control of the speed and pressure of the nozzle, as well as the temperature and composition of the materials used. Specifically, rheological behavior is crucial to the formation of droplets in inkjet bioprinting.<sup>57</sup> Therefore, only materials with a viscosity range of 10 mPa·s are considered suitable.<sup>58,59</sup> For instance, cell-laden hydrogels, such as collagen or fibrin, are not suitable for inkjet bioprinting, as their high viscosity (up to 10,000 mPa·s) does not permit the formation of droplets. In contrast, low-viscosity materials such as alginate- or polyethylene glycol (PEG)-based hydrogels (1–2 mPa·s) can be used in inkjet bioprinting, but they require the addition of crosslinkers to increase the viscosity to the appropriate range. Non-Newtonian fluids are most appropriate for extrusion-based bioprinting. For example, thermally sensitive and shear-thinning hydrogels such as alginate can be extruded with high resolution and accuracy due to their low viscosity at low shear rates.<sup>60</sup> As a result, bioink printability can sometimes be contrasted with bioink formulations, and it is impossible to maintain its printability parallel to mechanically optimized features.

The bioink must possess both thixotropic and extrudability characteristics, which determine whether it can be continuously squeezed out of the bioprinting nozzles. These attributes become critical when extra force is needed for hydrogel extrusion, which could diminish cellular viability.<sup>61,62</sup> For instance, to ensure the highest viability of printed cells, the extrusion pressure must be below the threshold value of 1.5 kPa. Additionally, current bioprinters are primarily designed to dispense liquid, or semiliquid materials, limiting the design of an ideal bioink with thixotropic properties.<sup>63</sup> Both thixotropic and extrudability properties directly limit the formulation of bioink and hinder the mechanical strength of the bioprinted

construct. For example, the use of high concentrations of hydrogel precursors, such as alginate, can result in a bioink with high mechanical strength, but this bioink is not extrudable due to its high viscosity.

Embedded cells in bioink influence its printability and indirectly determine its physical properties. Cells embedded in bioink reduce its viscosity, allowing it to be extruded through a 3D printer.<sup>64</sup> However, when the concentration of cells is too high, they can compromise the mechanical strength of the bioink. Therefore, it is critical to find a balance between cell concentration and hydrogel precursors in order to produce a bioink with both high mechanical strength and printability. As in a previous experiment conducted to compare the impact of the presence of hepatocarcinoma cells on the bioprinting of methacrylamide-modified gelatin (Gel-MOD), the rheological properties were modified, and the viscosity of the bioink changed along with the incorporation of the cells.<sup>65</sup> Also, Diamantides *et al.*<sup>66</sup> have investigated the influence of cell density on the rheological and printability properties of collagen bioink, illustrating that moderate cell density could improve printability. Furthermore, the capability to maintain the structural integrity of a bioprinted construct with increasing cell density requires an in-depth understanding of the material properties of the bioinks. Thus, any agent that manipulates the formulation of bioink could directly impact its printability and restrict cellular viability. As such, the formulation of bioink must be carefully designed to enable successful bioprinting and ensure cell viability.

#### 4. Application-specific requirements for bone bioprinting

The clinical translation of bone bioprinting technology requires consideration of diverse application circumstances, each presenting unique mechanical, biological, and structural requirements. Understanding these demands is essential for designing appropriate bioinks and fabrication strategies.<sup>75</sup>

Critical-sized bone defects represent the most mechanically demanding application scenario. These defects, typically beyond 2–3 cm in long bones, result from trauma, tumor resection, osteomyelitis, or nonunion fractures. Bioprinted constructs for these applications must exhibit high compressive strength (100–200 MPa) to bear immediate load-bearing requirements, incorporate proangiogenic factors to support vascularization, and demonstrate controlled degradation kinetics that match new bone formation rates.<sup>75</sup> Recent studies have shown that composite scaffolds combining biodegradable polymers with bioceramics can achieve the necessary mechanical standards while supporting cell viability and osteogenic differentiation.<sup>76</sup>

Craniofacial reconstruction applications, including mandibular defects and calvarial reconstruction, focus on precise anatomical replication and mechanical function. These purposes typically require moderate mechanical properties (50–150 MPa compressive strength) but demand high geometric accuracy and smooth surface.<sup>77</sup> Patient-specific 3D-bioprinted constructs based on computed

**Table 1. Main challenges to mechanically optimized hydrogels bioprinting**

Limitation	Description	Ideal condition for printing	Possible solution	Acceptable range	Refs.
Viscosity	Hydrogels with high viscosity are difficult to print because they do not flow easily through the printer nozzle.	Low viscosity	Use a printing nozzle with a larger diameter or reduce the viscosity of the hydrogel by adding diluents or using lower-molecular-weight polymers.	100–10,000 Pa·s	67,68
Shear stress tolerance	Hydrogels with low shear stress tolerance are easily damaged when they are subjected to the shear stress of printing.	Low shear stress	Use a printing method with lower shear stress, such as extrusion printing or drop-on-demand printing.	0.1–10 Pa	69,70
Gelation speed	Hydrogels with fast gelation speeds may subject to very rapid solidification during printing, which can lead to clogging of the printer nozzle.	Slow gelation speed	Use a hydrogel with a slower gelation speed or reduce the gelation speed by adjusting the crosslinking conditions.	1–60 min	71,72
Printability resolution	Hydrogels with low printability resolution cannot be used to print constructs with fine details.	High printability resolution	Use a printing method with high resolution, such as stereolithography (SLA) or digital light processing (DLP).	50–500 μm	73,74

tomography (CT) imaging have demonstrated superior outcomes compared to conventional approaches by enabling precise anatomical fit.<sup>78</sup> Multimaterial bioprinting creates gradient scaffolds with cortical-like regions transitioning to trabecular-like zones, recapitulating bone's mechanical heterogeneity.<sup>79,80</sup>

Osteochondral tissue engineering presents unique challenges due to the need for gradient structures mimicking the transition from articular cartilage to subchondral bone. This application requires bioprinting of stratified constructs with spatially varying mechanical properties<sup>81</sup>: soft hydrogels (0.5–2 MPa)<sup>82</sup> for the cartilage layer, hydrogels with intermediate stiffness (1–10 MPa)<sup>83</sup> for the calcified cartilage zone, and stiffer substrate (10–20 MPa)<sup>84</sup> for subchondral bone. Dynamic mixing during printing creates seamless transitions, reducing delamination, and improving interfacial integration in *in vivo* models.<sup>85</sup> Organoid-integrated bioprinted constructs combine self-organized tissue structures (diameter 200–500  $\mu\text{m}$ ) with hydrogel matrices. Bone organoids demonstrate enhanced mineralization, elevated osteogenic markers and superior performance in osteochondral defect models compared to dissociated cell approaches.<sup>86</sup>

Osteoporotic fracture treatment requires bioprinted constructs that can integrate with mechanically compromised host bone which have reduced mineral density and altered microarchitecture. These applications benefit from bioinks incorporating osteo-promotive factors, such as bone morphogenetic proteins, parathyroid hormone (PTH) peptides, or bisphosphonates that stimulate both construct integration and host bone architecture improvement.<sup>87</sup> Mechanical properties should match the weakened host bone (5–10 MPa) to minimize stress shielding while providing adequate structural support.<sup>88</sup>

Understanding these application-specific requirements enables rational design of bioinks, scaffold architectures, and fabrication strategies tailored to clinical needs, ultimately advancing the translational potential of bone bioprinting technology.

## 5. Strategies to overcome mechanical challenges

Despite the variety of materials used in the production of bioinks, it seems that without additives, their drawbacks may still compromise their usage. As a result, developing new scaffolds with improved mechanical strength can be fulfilled by adding other materials and creating composite constructs. Several studies have focused on developing new composite scaffolds to promote mechanical properties for bone tissue engineering. In this section, different

approaches for improving the mechanical properties of 3D-printed constructs will be discussed (Figure 3).

### 5.1. Developing composite constructs

#### 5.1.1. Incorporation of bioceramic/polymer composite

A composite scaffold consisting of calcium phosphate and collagen developed using low-temperature 3D printing possesses desirable cytocompatibility, mechanical strength, and bone regeneration in a critical-sized femoral defect. By optimizing the concentration of phosphoric acid-based binder solution and supplemented collagen solution, appropriate cytocompatibility and mechanical strength were achieved. The addition of collagen to the binder solution increases the strength of the 3D-printed construct in a linear fashion, with higher collagen concentrations resulting in stronger constructs. By increasing the concentration of collagen in the solution (0–2 wt%), the maximum flexural strength could improve from 55 to 75 kPa. Implantation of such 3D-printed scaffold into a critical-sized murine femoral defect resulted in a desirable new bone formation.<sup>89</sup> In another study, a composite hydrogel containing alginate, polyvinyl alcohol (PVA) and hydroxyapatite (HA) with optimal rheological properties and appropriate osteoconductivity was designed for reconstruction of bone defects. The addition of HA into alginate-PVA solution enhanced the viscosity of hydrogel and simultaneously promoted the osteoconductivity of the printed scaffold. This optimized formulation represented a storage modulus of 600–1200 Pa following gelation, as depicted by rheological assessments. Moreover, the selected hydrogel revealed the average compressive modulus of 10.3 kPa and this value was continually decreased to 2.4 kPa over 14 days of immersion in culture medium. Encapsulation of mouse calvaria 3T3-E1 (MC3T3) cells within optimal hydrogel exhibited well distribution and high viability through the process of 3D printing.<sup>60</sup>

#### 5.1.2. Addition of inorganic nanofillers

Nanosilicate (nSi) may also be considered as a promising biomaterial, which can be used in composite formation due to its biocompatibility and osteoinductivity features. A biomimetic nanocomposite bioink consisting of gelatin, alginate and nSi was developed for 3D bioprinting of engineered bone constructs. Incorporation of nSi considerably promoted the printability and mechanical strength of the printed constructs and improved the osteogenic differentiation of encapsulated rat bone marrow MSCs without any exogenous osteoinductive factors. Nanocomposite bioink with different concentrations of nSi (0–3%) was evaluated through a uniaxial compression test. Nanocomposites containing 2% and 3% nSi represented significantly higher compressive modulus ( $101.41 \pm 3.11$  kPa for 2% nSi and  $123.59 \pm 2.10$  kPa for 3% nSi) in

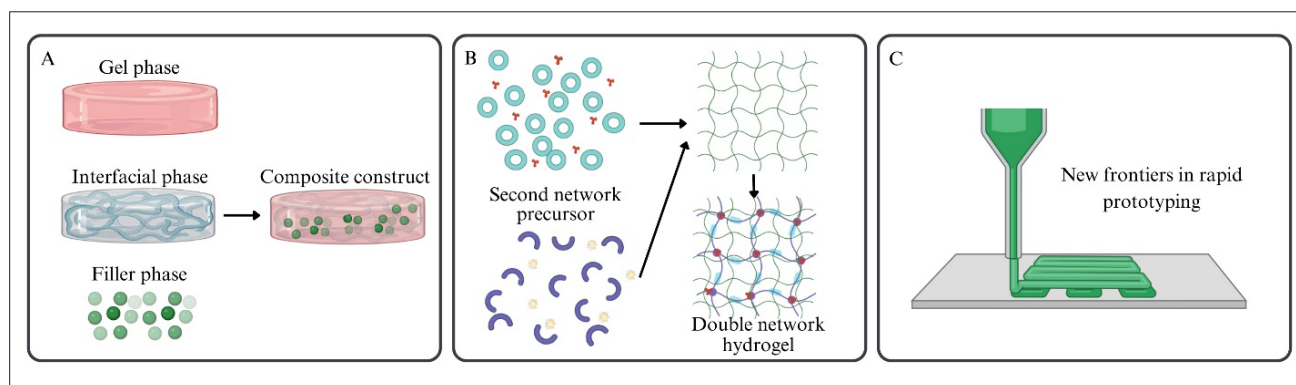


**Figure 3.** Different approaches for overcoming mechanical challenges in 3D bioprinting. (A) Introducing novel composite hydrogel with improved mechanical features; (B) Designing double-network hydrogel; (C) Developing an emerging technology for rapid prototyping of hydrogel.

comparison with 0% and 1% nSi ( $46.98 \pm 1.54$  kPa for 0% nSi and  $57.82 \pm 1.69$  kPa for 1% nSi). The results of rheological and mechanical analysis revealed that the addition of nSi considerably improved the printability of nanocomposite compared to gelatin-alginate alone, and increasing the concentration of the nSi promoted the mechanical strength of the constructs.<sup>90</sup> In an attempt to create a 3D-printed osteogenic nanocomposite, an alginate dialdehyde-gelatin (ADA-GEL) hydrogel containing mesoporous silica-calcia nanoparticles (MSNs) along with icariin drug was developed. Incorporation of MSNs promoted the mechanical stiffness of the constructs as well as cell adhesion and proliferation, as a result of inducing apatite layer formation following immersion in simulated body fluid. The nanocomposite hydrogels represented considerably higher stiffness compared to the neat hydrogel ( $60 \pm 15$  kPa for ADA-GEL/MSN vs.  $25 \pm 10$  kPa for ADA-GEL). The covalent interaction between flexible hydrogel and stiff MSNs results in higher stiffness of the hydrogel nanocomposite. Interestingly, the hydrogel nanocomposites containing icariin depicted higher compressive stiffness ( $160 \pm 40$  kPa) compared to the neat hydrogel. In these nanocomposites, numerous hydroxyl groups of icariin provide hydrogen bonding with amine groups of gelatin. Moreover, esterification may take place due to the interactions of the hydroxyl groups from icariin and carboxyl groups of gelatin and consequently result in higher mechanical stiffness of icariin-containing hydrogel nanocomposites. Furthermore, it has been shown that such hydrogel nanocomposites improve osteoblast proliferation, adhesion, and differentiation.<sup>91</sup>

In a comparative experiment, osteogenic differentiation, printability, and physiochemical features of common alginate-based bioinks, including alginate-nanocellulose (alg-ncel), alginate- $\text{CaCl}_2$  (alg- $\text{CaCl}_2$ ), alginate-gelatin (alg-gel), and alginate- $\text{CaSO}_4$  (alg- $\text{CaSO}_4$ ) have been analyzed.

Among bioinks, alg- $\text{CaSO}_4$  and alg-ncel represented higher storage modulus in comparison with alg- $\text{CaCl}_2$  and alg-gel constructs ( $9.9 \pm 4.9$  kPa for alg- $\text{CaSO}_4$ ,  $7.1 \pm 0.6$  kPa for alg-ncel,  $4.1 \pm 0.6$  kPa for alg- $\text{CaCl}_2$ , and  $2.6 \pm 1.1$  kPa for alg-gel). After 7 days in culture, all hydrogels showed declines in stiffness except for the alg-ncel group, which preserved its stability. The reduction in stiffness in the alg- $\text{CaCl}_2$  and alg- $\text{CaSO}_4$  constructs following 7 days in culture may be attributed to the dissociation of calcium crosslinks. Encapsulation of MSCs in alg- $\text{CaCl}_2$  constructs during culture in the osteogenic medium revealed more osteogenic differentiation compared to the other three bioinks mentioned above.<sup>92</sup>

## 5.2. Developing double-network hydrogels

Double-network hydrogels represent an advanced biomaterial design strategy wherein two interpenetrating polymer networks with distinct crosslinking mechanisms synergistically contribute to mechanical performance. The mechanical superiority of double-network hydrogels derives from their capacity to distribute stress across both networks, with the sacrificial bonds in the first network rupturing preferentially to absorb energy, while the second network maintains overall structural continuity. Recent innovations have focused on incorporating dynamic and reversible crosslinks that enable stress relaxation while maintaining mechanical robustness.<sup>93</sup>

A double-network hydrogel composed of alginate, methacrylated gelatin (GelMA), and polyethylene glycol diacrylate (PEGDA) was developed as a 3D-bioprinted construct for bone reconstruction. Calcium-crosslinked alginate and created a physical network while PEGDA/GelMA formed a chemical network through covalent crosslinking. This unique double network structure provided stretchability in the bioink and enabled desirable strength and stiffness for bone remodeling. The results of

the compression test revealed that the double-network bioink possesses a compressive modulus of 78.1 kPa, strength of 60.4 kPa, strain at break of 33.9%, and toughness of 71.35 kJ/m<sup>3</sup>.<sup>94</sup>

In another study, a double-network hydrogel composed of polyurethane (PU) and gelatin with adjustable mechanical features and degradation rates was prepared as bioink. The two-stage double-network structure was formed via Ca<sup>2+</sup> chelation and thermal gelation at 37°C. The PU-gelatin double-network hydrogel possessed desirable elasticity and mechanical strength and could promote MSC proliferation. The biodegradable waterborne PU was the major constituent of this bioink and provided the essential elasticity, tunable mechanical characteristics, as well as shear thinning feature. However, PU possessed low viscosity, which hampered its printability. Therefore, gelatin was incorporated to improve the viscosity of bioink and provided the stability of printed construct. At room temperature, the static compressive modulus (1.5 ± 0.2 kPa), strength (5.2 ± 0.6 kPa), and deformation (69.6 ± 6.1%) of PU-gelatin hydrogel after the CaCl<sub>2</sub> treatment was higher than hydrogel without CaCl<sub>2</sub> treatment (static compressive modulus of 0.6 ± 0.1 kPa, strength of 1.3 ± 0.2 kPa, and deformation of 62.3 ± 4.2%). At 37°C, however, the mentioned parameters were 2.6 ± 0.3 kPa, 8.1 ± 1.1 kPa, and 68.8 ± 8.3%, respectively. Moreover, the static tensile modulus (14.7 ± 1.3 kPa), strength (7.3 ± 0.6 kPa), and elongation (105 ± 10.8%) of PU-gelatin hydrogels following 24 h of incubation were significantly higher than the hydrogels before incubation (static tensile modulus of 7.2 ± 0.8 kPa, strength of 3.2 ± 0.3 kPa, and elongation of 94.1 ± 10.3%).<sup>95</sup>

Bone-derived decellularized ECM (dECM) integrated into alginate networks presents another promising double-network strategy that combines mechanical enhancement with biological functionality. An alginate-methacrylated dECM (Alg/Ma-dECM) system demonstrated considerably higher compressive modulus (90.4 ± 14.9 kPa) compared to alginate-CaCl<sub>2</sub> hydrogel alone (35.6 ± 8.9 kPa). The improvement in mechanical properties was attributed to the presence of UV-crosslinked Ma-dECM constituent in printed constructs, creating a hybrid physical-chemical crosslinking network. Importantly, the dECM component provided growth factors and ECM proteins that promoted cell adhesion, proliferation, and osteogenic differentiation beyond purely mechanical benefits.<sup>96</sup>

DNA-encoded dynamic hydrogels represent a cutting-edge approach for organoid bioprinting, leveraging the programmable and reversible nature of DNA base pairing to create networks with precisely tunable mechanical properties and stress relaxation kinetics. These systems

utilize complementary DNA sequences as dynamic crosslinkers that can repeatedly associate and dissociate, enabling cellular remodeling and mechanoadaptation. For cartilage organoid bioprinting, DNA-silk fibroin (DNA-SF) hydrogel sustained-release systems have achieved remarkable success, supporting development of millimeter-scale organoids with authentic cartilage phenotypes. The programmability of DNA crosslinks enables rational design of stress relaxation timescales matching cellular contractile dynamics (seconds to minutes), facilitating cell spreading, migration, and tissue organization.<sup>97</sup> The mechanical properties, crosslinking mechanisms, and their limitations characteristics of the double-network hydrogel systems discussed in this section are summarized in Table 2.

### 5.3. Rapid prototyping technology

The various strategies were investigated to develop 3D-bioprinted constructs with desirable mechanical properties for bone regeneration. The scaffolds derived from natural polymers are mechanically weak; therefore, incorporation of inorganic additives may improve mechanical strength and also bioactivity. These materials are printed together with living cells, achieving simultaneous cellular encapsulation and mechanical reinforcement. The incorporation of nanohydroxyapatite (nHAp) and bioactive glass nanoparticles (BGNp) into alginate/gelatin bioinks operates through multiple reinforcement mechanisms. First, the ceramic nanofillers provide direct physical reinforcement through load-bearing interactions within the hydrogel network. Second, nanoparticles serve as nanoscale crosslinking sites, establishing electrostatic interactions with polymer chains and increasing network density. Third, the ceramic nanoparticles release bioactive ions (Ca<sup>2+</sup>, PO<sub>4</sub><sup>3-</sup>, Si<sup>4+</sup>) that promote both ionic crosslinking of the hydrogel matrix and osteogenic differentiation of encapsulated cells.<sup>98,99</sup> When bioprinted using extrusion-based bioprinting systems, these nanocomposite bioinks achieve compressive moduli of 80–150 kPa (compared to 5–10 kPa for unreinforced alginate/gelatin hydrogels), sustained cell viability exceeding 85% postprinting, and improved shape fidelity during and after printing. The nanoparticles create hierarchical interactions with polymer chains, enabling the bioink to maintain high viscosity at low shear rates in the syringe before extrusion while dramatically reducing apparent viscosity during nozzle extrusion.<sup>100</sup> This combination minimizes shear stress experienced by cells while maintaining strand integrity postextrusion.

To achieve both immediate structural stability critical for handling complex printed geometries and long-term mechanical integrity, recent bioprinting approaches employ dual-crosslinking strategies that combine

**Table 2. Comparison of double-network hydrogel systems for bone bioprinting**

Network components	Crosslinking mechanisms	Compressive modulus	Limitations	Refs.
Alginate (physical), PEGDA/ GelMA (chemical)	Ionic (Ca <sup>2+</sup> ), photopolymerization	78.1 kPa	Moderate strength, potential phototoxicity	94
PU (chemical), gelatin (physical)	Covalent, Ca <sup>2+</sup> chelation, thermal	7.3 ± 0.6 kPa (37°C)	Lower stiffness, complex formulation	95
Alginate (physical), Ma-dECM (chemical)	Ionic (Ca <sup>2+</sup> ), photopolymerization	90.4 ± 14.9 kPa	Batch variation, limited strength	96
DNA crosslinks, silk fibroin	Programmable base-pairing, physical entanglement	Variable (tunable)	Cost, complexity, primarily for soft tissues	97

Abbreviations: GelMA: Gelatin methacrylate; Ma-dECM: Methacrylated decellularized extracellular matrix; PEGDA: Polyethylene glycol diacrylate; PU: Polyurethane.

chemical and ionic crosslinking. Representative dual-crosslinked bioink compositions include alginate (2–3% w/v) providing the backbone for ionic crosslinking, GelMA (8–10% w/v) with methacrylate groups enabling photochemical crosslinking, gellan gum (0.5–1% w/v) enhancing shear-thinning properties, hydroxyapatite nanoparticles (10–15% w/v) providing osteogenic reinforcement, and cell suspensions of SaOS-2 osteoblasts or hBMSCs at  $2 \times 10^6$  cells/mL. Following 3D bioprinting via extrusion bioprinting, constructs are immediately exposed to ultraviolet (UV) irradiation to induce free-radical polymerization of the methacrylate groups on GelMA, forming covalent C–C bonds between polymer chains and establishing a primary photochemical network. Constructs are subsequently immersed in calcium chloride solution, where Ca<sup>2+</sup> ions form ionic bridges between guluronate and mannuronate blocks of the alginate polymer and simultaneously crosslink gellan gum polymer chains, establishing a secondary ionic network. The dual-crosslinked networks create robust hydrogel structures with compressive strength ranging from 200 to 400 kPa, featuring increased elasticity while maintaining structural integrity despite cell-mediated extracellular matrix remodeling during culture.<sup>101,102</sup> Furthermore, these dual-crosslinked networks exhibit enhanced stability in physiological conditions demonstrating minimal scaffold degradation, which is crucial for supporting long-term cellular function and tissue development.

A paradigm-shifting approach addresses the critical challenge of achieving bone-level mechanical strength (>500 kPa) while maintaining cell viability during bioprinting. The optimized gelatin methacryloyl/laponite nanoclay/*N*-acryloyl glycinamide (GLN) bioink achieves exceptional mechanical properties with compression modulus of  $989 \pm 49$  kPa and compression strength of  $1200 \pm 78$  kPa. This bioink enables one-step coaxial extrusion bioprinting of hollow hydrogel-based scaffolds (HHS) with tunable architecture (outer diameter 0.4–0.8 mm, inner

diameter 0.1–0.6 mm) that can be printed acellularly then loaded postfabrication with 13-fold increased cell loading efficiency, >85% cell viability and uniform cell distribution. The hollow scaffold architecture allows precise spatial segregation of multiple cell types: endothelial cells (HUVECs) populate the hollow channels, forming interconnected vascular networks with a mature endothelial phenotype, while osteogenic cells (hBMSCs) seeded on the solid walls undergo osteogenic differentiation. In critical-sized segmental rat femoral defects (8 mm), HHS-loaded hBMSCs accomplished complete bridging by 12 weeks with 2.1-fold higher new bone volume compared to acellular scaffolds, while HHS-loaded with both hBMSCs and HUVECs demonstrated 2.5-fold higher bone volume with enhanced early vascularization preceding bone formation. Also, in osteoporotic metaphyseal defects, HHS-loaded with hBMSCs achieved robust bone regeneration despite the osteoporotic host environment, demonstrating that cell-laden constructs overcome both the mechanical insufficiency of purely acellular scaffolds and the biological insufficiency of osteoporotic host tissues.<sup>103</sup>

## 6. Osteo-promotive materials and their roles

Recent investigations have been focused on discovering and utilizing osteo-promoting factors that facilitate the new bone formation and can be used in the preparation of mechanically enhanced scaffolds. In parallel with bone formation, ECM components, dECM particles, and nanoparticles may act as osteo-promoting agents (Table 3). The ECM consists of a network of proteins and polysaccharides that offer an appropriate binding site for growth factors, cytokines, and other molecules involved in bone formation. It allows cells to interact with one another and with the surrounding environment, therefore stimulating osteoblast differentiation. Components of the ECM could also deliver a substrate and a physically

supportive environment for new bone arrangements. The ECM components have been shown to interact with osteoblasts and enhance their survival, proliferation, and differentiation.<sup>104</sup> This leads to increased matrix deposition and consequently reinforces the mechanical strength of the resulting construct. The ECM component can be used in combination with biomaterials to create mechanically enhanced bioinks. For instance, the addition of collagen to a nHAp-based bioink was demonstrated to improve the interconnectivity of the formed construct and its mechanical properties.

Decellularized human ECM could be a promising osteo-promotive material because of its similarity to native bone tissue. It was demonstrated that osteogenic MSC-derived ECM could stimulate osteogenic differentiation and mineralization.<sup>105</sup> Moreover, a comparative experiment between autogenous bone pieces, intramembranous demineralized bone matrix (DBM), and HA was carried out to investigate the mechanical strength of healed rat calvarial defects, trephined into the parietal bones, and then filled with the mentioned materials. The results showed that the defects filled with DBM had better mechanical strength than defects implanted with HA or bone pieces.<sup>106</sup> Although these results have validated the remarkable characteristics of ECM-based biomaterials, batch-to-batch variation hinders their therapeutic application. To address this issue, recent studies have focused on developing standardized decellularization protocols to reduce variability. For example, an automated multitissue decellularization method has been developed to produce ECM biomaterials with reduced batch-to-batch variability, enhancing reproducibility and clinical applicability.<sup>107</sup> Additionally, the use of induced pluripotent stem cells (iPSCs) as a source for cell-secreted ECM has been proposed to offer scalability and potentially decrease batch-to-batch variations that hinder the clinical translation of ECM-based biomaterials. iPSCs can provide a consistent and renewable source of ECM, which may lead to more reproducible outcomes in tissue engineering application.<sup>108</sup>

Incorporating nanoscale materials to provide mechanically enhanced bioinks has offered another opportunity. The osteogenic efficacy and mechanical properties of injectable platelet-rich fibrin (i-PRF) scaffolds can be further enhanced through the addition of laponite, a synthetic nanosilicate clay with disc-shaped morphology (diameter ~25 nm, thickness ~1 nm). The compressive modulus of i-PRF-alginate/gelatin scaffolds increases from approximately 130 kPa to over 200 kPa with the addition of 1% laponite. Also, laponite forms electrostatic interactions with growth factors, enabling their controlled release over extended periods (>14 days), and it releases

bioactive ions ( $Mg^{2+}$ ,  $Si^{4+}$ ) that directly stimulate osteogenic differentiation.<sup>109</sup> Deng *et al.*<sup>110</sup> reported that polydopamine nanoparticles (PDA NP) were incorporated into fibrous membranes derived from polymerization of dopamine mixed with polycaprolactone (PCL). PDA NP in hybrid membranes, even without added growth factors, promoted osteogenic differentiation and supported MSC cytocompatibility, and successfully induced bone regeneration in mouse models of calvarial critical-sized defects.<sup>110</sup> Furthermore, PDA NP in hybrid membranes has been demonstrated to possess superior osteogenic activity compared to membranes without PDA NP. Metal nanoparticles, such as alloyed silver-platinum nanoparticles (AgPt NP), exhibit osteo-promotive properties, and cross-sectional focused-ion beam analysis has shown that they are internalized by hMSCs, exhibiting low cytotoxicity and antimicrobial activity while simultaneously promoting osteogenic differentiation.<sup>8</sup> Despite their osteopromotive and antimicrobial properties, potential cytotoxic effects of metal nanoparticles, such as silver-platinum nanoparticles (AgPt NPs), at high doses and concentrations must be considered. Studies have shown that AgPt NPs with a silver content above 50 mol% can release silver ions, leading to cytotoxicity in hMSCs. This cytotoxicity is attributed to the dissolution of silver ions from nanoparticles, which can induce oxidative stress and compromise cell viability.<sup>111</sup> Additionally, the cytotoxicity of bimetallic AgPt NPs has been found to be higher than that of monometallic silver nanoparticles. For instance, Ag70Pt30 and Ag50Pt50 nanoparticles exhibited significant cytotoxic effects on HeLa cells at concentrations around 50  $\mu g/mL$ . This increased toxicity is not solely due to silver ion release, suggesting that the combined presence of silver and platinum in the nanoparticle structure contributes to enhanced cytotoxic effects.<sup>112</sup> These AgPt NP were found to form a protective monolayer on the surface of hMSCs, which then triggered the secretion of osteogenic cytokines and proteins, such as osteocalcin, alkaline phosphatase, and osteopontin. This resulted in increased osteogenic differentiation of hMSCs, enhancing the expression of osteogenic markers and stimulating bone formation. Moreover, the use of nanoglass paste can help with generating new bone in a recent approach, where 200-nm-sized silicate-glass (with Ca, Cu) particles successfully induced osteogenic differentiation of MSCs and promoted angiogenesis.<sup>113</sup> This suggests that nanoparticles can be used to positively influence the osteogenic differentiation of hMSCs, ultimately leading to the production of new bones. Furthermore, they could augment osteoblast functionality and alkaline phosphatase (ALP) activity, consequently increasing the mechanical properties of the bioprinted constructs.

**Table 3. Osteo-promotive materials for bone-specific bioink optimization**

Candidate material	Mechanism of action	Printability	Disadvantages	Refs.
Hydroxyapatite (HA)	A mineral scaffold that promotes bone growth and mineralization, but can clog the printer nozzle at high concentrations	Printable using a variety of methods, but requires careful handling to prevent clogging	Sterilization challenging, as HA can be damaged by high temperatures and harsh chemicals	<sup>114</sup>
Bone morphogenetic proteins (BMPs)	Growth factors that promote the growth and differentiation of bone cells	Soluble BMPs can be easily incorporated into bioinks	BMPs can be degraded by enzymes in the body, limiting their therapeutic potential	<sup>115</sup>
Collagen	A natural scaffold that provides structure and support for bone cells	A challenging bioink ingredient to print with, as collagen is highly viscous	Collagen could be denatured by the shear stress of printing	<sup>116</sup>
Decellularized extracellular matrix (dECM)	Contains all the essential proteins and molecules for bone regeneration	A complex bioink ingredient that requires careful optimization to print without damaging the ECM	Sterilization can be challenging, as dECM is sensitive to heat and chemicals	<sup>104</sup>
Demineralized bone matrix (DBM)	A bioink ingredient that contains osteo-inductive factors that promote bone growth and differentiation	A versatile bioink ingredient that can be printed using a variety of methods, but requires careful handling	DBM variability can make it difficult to produce consistent results with DBM bioinks	<sup>117</sup>
Polydopamine nanoparticles (PDA NPs)	Nanoparticles that deliver osteo-inductive factors to bone cells and create scaffolds that support bone growth	PDA NPs can be printed at high resolutions, which is important for creating complex bone-shaped scaffolds	PDA NPs can be cytotoxic to cells at high concentrations	<sup>118</sup>
Silver–platinum nanoparticles ( <i>AgPt NPs</i> )	Nanoparticles that kill bacteria and promote bone growth	<i>AgPt NPs</i> can be incorporated into bioinks at high concentrations without clogging the printer nozzle	<i>AgPt NPs</i> can be expensive to produce at scale	<sup>119</sup>
Silicate-glass	Particles that deliver Ca and Cu ions to bone cells, which are essential for bone mineralization	Easily printable but requires careful optimization to avoid damaging the particles	Silicate-glass particles can form aggregates, which can lead to nozzle clogging of the bioprinter	<sup>120</sup>

## 7. Conclusion and future perspectives

At present, experimental studies for developing the ideal formulation for bone bioink are in progress. Over the past few years, relevant research has focused on improving different criteria of bioinks. However, significant challenges remain, including achieving compressive strength equivalent to natural bones, replicating complex geometries, maintaining appropriate porosity without compromising other features or properties, and promoting vascularization to support cell survival.<sup>121</sup> To surmount these challenges, various solutions have been attempted, including developing composite hydrogels to fulfill the goal of enforcing mechanical strength and printability, as well as preserving the encapsulated cells in the bioprinting process. Moreover, biodegradability of the constructs has been achieved through the use and development of new formulations.<sup>122</sup> Printing methods and appliances, such as nozzle-based or laser-based printers, with the help of computer-aided design (CAD), have also played an essential role in revolutionizing the production of artificial

scaffolds. Other challenges, such as bioink preparation, cell viability and differentiation, and angiogenesis inside the scaffolds require further investigation. Ultimately, it is important to not only sort out the mentioned limitations, but also to reduce the cost of final constructs. Currently, angiogenesis within the scaffolds is stimulated using approaches such as nonviral gene delivery and nanoparticles<sup>123</sup>; however, these strategies have raised ongoing concerns regarding the potential activation of proto-oncogenes and tumorigenesis.<sup>124</sup> Overall, given the increasing demand for 3D-bioprinted constructs driven by high transplantation failure rates and limited availability of donor organs and tissues, there is a pressing need to develop new strategies to address these challenges.

The current review revolves around existing strategies for addressing mechanical challenges, which are primarily addressed by the development of composite bioinks and the optimization of scaffold architecture. While these approaches have shown promise, they are often associated with a trade-off between mechanical

strength and biocompatibility. The next generation of bioprinted bone constructs is expected to embrace a “dynamic mechanoregulation” paradigm, in which scaffold mechanical properties are not static but can be adjusted *in situ* to match the changing needs of regenerating tissue. This will be achieved through the development of “smart” bioinks that can respond to specific biological or physical cues, and the use of advanced bioreactors that can apply controlled mechanical stimuli to the developing construct. Ultimately, the goal is to create a truly living implant that can actively participate in the process of bone regeneration, rather than simply acting as a passive scaffold.

## Acknowledgments

None.

## Funding

The authors did not receive support from any organization for the submitted work.

## Conflict of interest

The authors declare that they have no competing interests.

## Author contributions

*Conceptualization:* Amin Ebrahimi Sadrabadi, Mohamadreza Baghaban Eslaminejad, Samaneh Hosseini

*Visualization:* Yalda Alibeigian

*Writing–original draft:* Amin Ebrahimi Sadrabadi, Payam Baei

*Writing–review & editing:* Mohamadreza Baghaban Eslaminejad, Samaneh Hosseini,

## Ethics approval and consent to participate

Not applicable.

## Consent for publication

Not applicable.

## Availability of data

The resources that support this review work are available upon request from the corresponding author.

## References

- Chimene D, Lennox KK, Kaunas RR, Gaharwar AK. Advancedbioinks for 3d printing: a materials science perspective. *Ann Biomed Eng.* 2016;44(6):2090-2102. doi: 10.1007/s10439-016-1638-y
- Pedroza-Gonzalez SC, Rodriguez-Salvador M, Perez-Benitez BE, Alvarez MM, Santiago GT. Bioinks for 3D bioprinting: a scientometric analysis of two decades of progress. *Int J Bioprint.* 2021;7(2):333. doi: 10.18063/ijb.v7i2.337
- Engler AJ, Sen S, Sweeney HL, Discher DE. Matrix elasticity directs stem cell lineage specification. *Cell.* 2006;126(4):677-689. doi: 10.1016/j.cell.2006.06.044
- Chaudhuri O, Gu L, Klumpers D, *et al.* Hydrogels with tunable stress relaxation regulate stem cell fate and activity. *Nat Mater.* 2016;15(3):326-334. doi: 10.1038/nmat4489
- Bergonzi C, Bianchera A, Remaggi G, Ossiprandi MC, Bettini R, Elviri L. 3D printed chitosan/alginate hydrogels for the controlled release of silver sulfadiazine in wound healing applications: design, characterization and antimicrobial activity. *Micromachines (Basel).* 2023;14(1):137. doi: 10.3390/mi14010137
- Wang L, Zhou A, Chen C, Huang X, Zhang S, Chen J. Preparation and properties of composite hydrogels for 3D bioprinting. *Polym Adv Technol.* 2023;34(7):2369-2383. doi: 10.1002/pat.6057
- Zhang X, Yang X, Wu W, *et al.* Improving the mechanical properties of 3D printed GelMA composite hydrogels by tannic acid. *MedComm–Biomater Appl.* 2023;2(3):e51. doi: 10.1002/mba.2.51
- Breisch M, Grasmik V, Loza K, *et al.* Bimetallic silver-platinum nanoparticles with combined osteo-promotive and antimicrobial activity. *Nanotechnology.* 2019;30(30):305101. doi: 10.1088/1361-6528/ab172b
- Lu N, Lu Y, Liu S, *et al.* Tailor-engineered POSS-based hybrid gels for bone regeneration. *Biomacromolecules.* 2019;20(9):3485-3493. doi: 10.1021/acs.biomac.9b00771
- Hoyle CE, Bowman CN. Thiol-ene click chemistry. *Angew Chem Int Ed Engl.* 2010;49(9):1540-1573. doi: 10.1002/anie.200903924
- Fairbanks BD, Schwartz MP, Halevi AE, Nuttelman CR, Bowman CN, Anseth KS. A versatile synthetic extracellular matrix mimic via thiol-norbornene photopolymerization. *Adv Mater.* 2009;21(48):5005-5010. doi: 10.1002/adma.200901808
- Mondal S, Lessard JJ, Meena CL, Sanjayan GJ, Sumerlin BS. Janus Cross-links in supramolecular networks. *J Am Chem Soc.* 2022;144(2):845-853. doi: 10.1021/jacs.1c10606
- Motloung MP, Mofokeng TG, Ray SS. Viscoelastic, thermal, and mechanical properties of melt-processed poly (epsilon-caprolactone) (PCL)/hydroxyapatite (HAP) composites. *Materials (Basel).* 2021;15(1):104.

- doi: 10.3390/ma15010104
14. Chuysinuan P, Nooeaid P, Thanyacharoen T, Techasakul S, Pavasant P, Kanjanamekanant K. Injectable eggshell-derived hydroxyapatite-incorporated fibroin-alginate composite hydrogel for bone tissue engineering. *Int J Biol Macromol.* 2021;193(Pt A):799-808. doi: 10.1016/j.ijbiomac.2021.10.132
  15. Stocco TD, de Carvalho RP, Silva HCO, de Melo Sousa TS. The feasibility of 3D bioprinting for bone regeneration: key challenges and future directions. *Regen Med.* 2025;20(11):625-652. doi: 10.1080/17460751.2025.2572218
  16. Garcia-Aznar JM, Nasello G, Hervas-Raluy S, Perez MA, Gomez-Benito MJ. Multiscale modeling of bone tissue mechanobiology. *Bone.* 2021;151:116032. doi: 10.1016/j.bone.2021.116032
  17. Chmielewska A, Dean D. The role of stiffness-matching in avoiding stress shielding-induced bone loss and stress concentration-induced skeletal reconstruction device failure. *Acta Biomater.* 2024;173:51-65. doi: 10.1016/j.actbio.2023.11.011
  18. Florencio-Silva R, Sasso GRdS, Sasso-Cerri E, Simões MJ, Cerri PS. Biology of bone tissue: structure, function, and factors that influence bone cells. *BioMed Res. Int.* 2015;2015(1):421746. doi: 10.1155/2015/421746
  19. Raubenheimer E, Miniggió H, Lemmer L, van Heerden W. The role of bone remodelling in maintaining and restoring bone health: an overview. *Clin. Rev. Bone Miner Metab.* 2017;15:90-97. doi: 10.1007/s12018-017-9230-z
  20. Hadjidakis DJ, Androulakis, II. Bone remodeling. *Ann N Y Acad Sci.* 2006;1092(1):385-396. doi: 10.1196/annals.1365.035
  21. Crockett JC, Rogers MJ, Coxon FP, Hocking LJ, Helfrich MH. Bone remodelling at a glance. *J Cell Sci.* 2011;124(7):991-998. doi: 10.1242/jcs.063032
  22. Ott SM. Cortical or trabecular bone: what's the difference? *Am J Nephrol.* 2018;47(6):373-375. doi: 10.1159/000489672
  23. Reyes KJC, Stanford FC, Singhal V, et al. Bone density, microarchitecture and strength estimates in white versus African American youth with obesity. *Bone.* 2020;138:115514. doi: 10.1016/j.bone.2020.115514
  24. Reichert JC, Wullschlegler ME, Cipitria A, et al. Custom-made composite scaffolds for segmental defect repair in long bones. *Int Orthop.* 2011;35(8):1229-1236. doi: 10.1007/s00264-010-1146-x
  25. Cheung AM, Adachi JD, Hanley DA, et al. High-resolution peripheral quantitative computed tomography for the assessment of bone strength and structure: a review by the Canadian Bone Strength Working Group. *Curr Osteoporos Rep.* Jun 2013;11(2):136-146. doi: 10.1007/s11914-013-0140-9
  26. Das D, Zhang S, Noh I. Synthesis and characterizations of alginate- $\alpha$ -tricalcium phosphate microparticle hybrid film with flexibility and high mechanical property as a biomaterial. *Biomed. Mater.* 2018;13(2):025008. doi: 10.1088/1748-605X/aa8fa1
  27. Abelardo E. Synthetic material bioinks. In: *3D Bioprinting for Reconstructive Surgery.* Amsterdam, Netherlands: Elsevier; 2018:137-144.
  28. Popp K, Xu C, Yuan A, et al. Trabecular microstructure is influenced by race and sex in Black and White young adults. *Osteoporosis Int.* 2019;30:201-209. doi: 10.1007/s00198-018-4729-9
  29. De Mori A, Pena Fernandez M, Blunn G, Tozzi G, Roldo M. 3D printing and electrospinning of composite hydrogels for cartilage and bone tissue engineering. *Polymers (Basel).* 2018;10(3):285. doi: 10.3390/polym10030285
  30. Morgan EF, Unnikrisnan GU, Hussein AI. Bone mechanical properties in healthy and diseased states. *Annu Rev Biomed Eng.* 2018;20(1):119-143. doi: 10.1146/annurev-bioeng-062117-121139
  31. Karpiński R, Jaworski Ł, Czubacka P. The structural and mechanical properties of the bone. *J Technol Exploitat Mech Eng.* 2017;3(1):43-51. doi: 10.35784/jteme.538
  32. Currey J. The structure and mechanical properties of bone. In: *Bioceramics and Their Clinical Applications.* Amsterdam, Netherlands: Elsevier; 2008:3-27.
  33. Vassiliou V, Chow E, Kardamakis D. *Bone Metastases: A Translational and Clinical Approach.* Vol 21. Dordrecht: Springer Science & Business Media; 2013.
  34. Shapiro F. Bone development and its relation to fracture repair. The role of mesenchymal osteoblasts and surface osteoblasts. *Eur Cell Mater.* 2008;15:53-76. doi: 10.22203/ecm.v015a05
  35. Kopperdahl DL, Keaveny TM. Yield strain behavior of trabecular bone. *J Biomech.* 1998;31(7):601-608. doi: 10.1016/s0021-9290(98)00057-8
  36. Currey JD. How well are bones designed to resist fracture? *J Bone Miner Res.* 2003;18(4):591-598. doi: 10.1359/jbmr.2003.18.4.591
  37. Osterhoff G, Morgan EF, Shefelbine SJ, Karim L, McNamara LM, Augat P. Bone mechanical properties and changes with osteoporosis. *Injury.* 2016;47 Suppl 2(Suppl 2):S11-S20. doi: 10.1016/S0020-1383(16)47003-8
  38. Boivin G, Bala Y, Doublier A, et al. The role of mineralization and organic matrix in the microhardness of

- bone tissue from controls and osteoporotic patients. *Bone*. 2008;43(3):532-538.  
doi: 10.1016/j.bone.2008.05.024
39. Bala Y, Farlay D, Boivin G. Bone mineralization: from tissue to crystal in normal and pathological contexts. *Osteoporos Int*. 2013;24(8):2153-2166.  
doi: 10.1007/s00198-012-2228-y
40. Zumstein V, Kraljević M, Wirz D, Hügli R, Müller-Gerbl M. Correlation between mineralization and mechanical strength of the subchondral bone plate of the humeral head. *J Shoulder Elbow Surg*. 2012;21(7):887-893.  
doi: 10.1016/j.jse.2011.05.018
41. Augat P, Schorlemmer S. The role of cortical bone and its microstructure in bone strength. *Age Ageing*. 2006;35 Suppl 2(suppl\_2):ii27-ii31.  
doi: 10.1093/ageing/af081
42. Zebaze RM, Ghasem-Zadeh A, Bohte A, et al. Intracortical remodelling and porosity in the distal radius and post-mortem femurs of women: a cross-sectional study. *Lancet*. 2010;375(9727):1729-1736.  
doi: 10.1016/S0140-6736(10)60320-0
43. Seeman E, Delmas PD, Hanley DA, et al. Microarchitectural deterioration of cortical and trabecular bone: differing effects of denosumab and alendronate. *J Bone Miner Res*. 2010;25(8):1886-1894.  
doi: 10.1002/jbmr.81
44. Riggs BL, Melton III LJ, Robb RA, et al. A population-based assessment of rates of bone loss at multiple skeletal sites: evidence for substantial trabecular bone loss in young adult women and men. *J Bone Miner Res*. 2008;23(2):205-214.  
doi: 10.1359/JBMR.07102
45. Luu YK, Pessin JE, Judex S, Rubin J, Rubin CT. Mechanical signals as a non-invasive means to influence mesenchymal stem cell fate, promoting bone and suppressing the fat phenotype. *Bonekey Osteovision*. 2009;6(4):132-149.  
doi: 10.1138/20090371
46. Guilak F, Cohen DM, Estes BT, Gimble JM, Liedtke W, Chen CS. Control of stem cell fate by physical interactions with the extracellular matrix. *Cell Stem Cell*. 2009;5(1):17-26.  
doi: 10.1016/j.stem.2009.06.016
47. Kirby TJ, Lammerding J. Cell mechanotransduction: stretch to express. *Nat Mater*. 2016;15(12):1227-1229.  
doi: 10.1038/nmat4809
48. Yang L, Gao Q, Ge L, et al. Topography induced stiffness alteration of stem cells influences osteogenic differentiation. *Biomater Sci*. 2020;8(9):2638-2652.  
doi: 10.1039/d0bm00264j
49. Shen B, Delaney MK, Du X. Inside-out, outside-in, and inside-outside-in: G protein signaling in integrin-mediated cell adhesion, spreading, and retraction. *Curr Opin Cell Biol*. 2012;24(5):600-606.  
doi: 10.1016/j.ceb.2012.08.011
50. Mousavi SJ, Doweidar MH. Role of mechanical cues in cell differentiation and proliferation: a 3D numerical model. *PLoS One*. 2015;10(5):e0124529.  
doi: 10.1371/journal.pone.0124529
51. Chowdhury F, Li Y, Poh YC, Yokohama-Tamaki T, Wang N, Tanaka TS. Soft substrates promote homogeneous self-renewal of embryonic stem cells via downregulating cell-matrix tractions. *PLoS One*. 2010;5(12):e15655.  
doi: 10.1371/journal.pone.0015655
52. Wang LS, Chung JE, Chan PP, Kurisawa M. Injectable biodegradable hydrogels with tunable mechanical properties for the stimulation of neurogenesis differentiation of human mesenchymal stem cells in 3D culture. *Biomaterials*. 2010;31(6):1148-1157.  
doi: 10.1016/j.biomaterials.2009.10.042
53. Zhang M, Sun Q, Liu Y, et al. Controllable ligand spacing stimulates cellular mechanotransduction and promotes stem cell osteogenic differentiation on soft hydrogels. *Biomaterials*. 2021;268:120543.  
doi: 10.1016/j.biomaterials.2020.120543
54. Cun X, Hosta-Rigau L. Topography: a biophysical approach to direct the fate of mesenchymal stem cells in tissue engineering applications. *Nanomaterials (Basel)*. 2020;10(10):2070.  
doi: 10.3390/nano10102070
55. Godoi FC, Prakash S, Bhandari BR. 3D printing technologies applied for food design: status and prospects. *J Food Eng*. 2016;179:44-54.  
doi: 10.1016/j.jfoodeng.2016.01.025
56. Hölzl K, Lin S, Tytgat L, Van Vlierberghe S, Gu L, Ovsianikov A. Bioink properties before, during and after 3D bioprinting. *Biofabrication*. 2016;8(3):032002.  
doi: 10.1088/1758-5090/8/3/032002
57. Hospodiuk M, Dey M, Sosnoski D, Ozbolat IT. The bioink: a comprehensive review on bioprintable materials. *Biotechnol Adv*. 2017;35(2):217-239.  
doi: 10.1016/j.biotechadv.2016.12.006
58. Saunders RE, Derby B. Inkjet printing biomaterials for tissue engineering: bioprinting. *Int Mater Rev*. 2014;59(8):430-448.  
doi: 10.1179/1743280414Y.0000000040
59. Xu T, Jin J, Gregory C, Hickman JJ, Boland T. Inkjet printing of viable mammalian cells. *Biomaterials*. 2005;26(1):93-99.  
doi: 10.1016/j.biomaterials.2004.04.011
60. Mancha Sanchez E, Gomez-Blanco JC, Lopez Nieto E, et al. Hydrogels for bioprinting: a systematic review of hydrogels synthesis, bioprinting parameters, and bioprinted structures behavior. *Front Bioeng Biotechnol*. 2020;8:776.  
doi: 10.3389/fbioe.2020.00776

61. Kyle S, Jessop ZM, Al-Sabah A, Whitaker IS. 'Printability' of candidate biomaterials for extrusion based 3D printing: state-of-the-art. *Adv Healthcare Mater.* 2017;6(16):1700264. doi: 10.1002/adhm.201700264
62. Li M, Tian X, Zhu N, Schreyer DJ, Chen X. Modeling process-induced cell damage in the biodepositing process. *Tissue Eng Part C Methods.* 2010;16(3):533-542. doi: 10.1089/ten.TEC.2009.0178
63. Aljohani W, Ullah MW, Zhang X, Yang G. Bioprinting and its applications in tissue engineering and regenerative medicine. *Int J Biol Macromol.* 2018;107(Pt A):261-275. doi: 10.1016/j.ijbiomac.2017.08.171
64. Shanjani Y, Pan CC, Elomaa L, Yang Y. A novel bioprinting method and system for forming hybrid tissue engineering constructs. *Biofabrication.* 2015;7(4):045008. doi: 10.1088/1758-5090/7/4/045008
65. Billiet T, Gevaert E, De Schryver T, Cornelissen M, Dubruel P. The 3D printing of gelatin methacrylamide cell-laden tissue-engineered constructs with high cell viability. *Biomaterials.* 2014;35(1):49-62. doi: 10.1016/j.biomaterials.2013.09.078
66. Diamantides N, Dugopolski C, Blahut E, Kennedy S, Bonassar LJ. High density cell seeding affects the rheology and printability of collagen bioinks. *Biofabrication.* 2019;11(4):045016. doi: 10.1088/1758-5090/ab3524
67. Gregory T, Benhal P, Scutte A, et al. Rheological characterization of cell-laden alginate-gelatin hydrogels for 3D biofabrication. *J Mech Behav Biomed Mater.* 2022;136:105474. doi: 10.1016/j.jmbbm.2022.105474
68. Guo Z, Ma C, Xie W, Tang A, Liu W. An effective DLP 3D printing strategy of high strength and toughness cellulose hydrogel towards strain sensing. *Carbohydr Polym.* 2023;315:121006. doi: 10.1016/j.carbpol.2023.121006
69. Müller SJ, Fabry B, Gekle S. Predicting cell stress and strain during extrusion bioprinting. *Phys Rev Appl.* 2023;19(6):064061. doi: 10.48550/arXiv.2209.13666
70. Boularaoui S, Shanti A, Khan KA, Iacoponi S, Christoforou N, Stefanini C. Harnessing shear stress preconditioning to improve cell viability in 3D post-printed biostructures using extrusion bioprinting. *Bioprinting.* 2022;25:e00184. doi: 10.1016/j.bprint.2021.e00184
71. Lyu J, Johnson M, Creagh-Flynn J, et al. Instant gelation system as self-healable and printable 3D cell culture bioink based on dynamic covalent chemistry. *ACS Appl Mater Interfaces.* 2020;12(35):38918-38924. doi.org/10.1021/acsmi.0c08567
72. Ashammakhi N, Ahadian S, Xu C, et al. Bioinks and bioprinting technologies to make heterogeneous and biomimetic tissue constructs. *Mater Today Bio.* 2019;1:100008. doi: 10.1016/j.mtbio.2019.100008
73. Schwab A, Levato R, D'Este M, Piluso S, Eglin D, Malda J. Printability and shape fidelity of bioinks in 3D bioprinting. *Chem Rev.* 2020;120(19):11028-11055. doi: 10.1021/acs.chemrev.0c00084
74. Oh D, Shirzad M, Kim MC, Chung EJ, Nam SY. Rheology-informed hierarchical machine learning model for the prediction of printing resolution in extrusion-based bioprinting. *Int J Bioprint.* 2023;9(6):308-324. doi: 10.36922/ijb.1280
75. Wu L, Zhao J, Huang J, Huang P, Zhao H. Advances and challenges in 3D bioprinting of bone organoids: materials, techniques, and functionalization strategies. *Int J Bioprint.* 2025;0(0) doi: 10.36922/ijb025190183
76. Khalaf AT, Wei Y, Wan J, et al. Bone tissue engineering through 3D bioprinting of bioceramic scaffolds: a review and update. *Life.* 2022;12(6):903. doi: 10.3390/life12060903
77. Lakatos E, Magyar L, Bojtár I. Material properties of the mandibular trabecular bone. *J Med Eng.* 2014;2014(1):470539. doi: 10.1155/2014/470539
78. Luo Y. Toward fully automated personalized orthopedic treatments: innovations and interdisciplinary gaps. *Bioengineering (Basel).* 2024;11(8):817. doi: 10.3390/bioengineering11080817
79. Zhou J, See CW, Sreenivasamurthy S, Zhu D. Customized additive manufacturing in bone scaffolds-the gateway to precise bone defect treatment. *Research (Wash D C).* 2023;6:0239. doi: 10.34133/research.0239
80. Varshney S, Dwivedi A, Pandey V. Bioprinting techniques for regeneration of oral and craniofacial tissues: current advances and future prospects. *J Oral Biol Craniofac Res.* 2025;15(2):331-346. doi: 10.1016/j.jobcr.2025.01.019
81. Lai Y, Fan J, Li P, et al. Recent advances in 3D bioprinting for cartilage and osteochondral regeneration. *Int J Bioprint.* 2025;0(0). doi: 10.36922/ijb025120098
82. Eschweiler J, Horn N, Rath B, et al. The biomechanics of cartilage: an overview. *Life (Basel).* 2021;11(4). doi: 10.3390/life11040302
83. Petitjean N, Canadas P, Royer P, Noel D, Le Floc'h S. Cartilage biomechanics: from the basic facts to the challenges of tissue engineering. *J Biomed Mater Res A.* 2023;111(7):1067-1089. doi: 10.1002/jbm.a.37478
84. Dąbrowski M, Rogala P, Uklejewski R, Patalas A, Winiecki M, Gapiński B. Subchondral bone relative area and density

- in human osteoarthritic femoral heads assessed with micro-CT before and after mechanical embedding of the innovative multi-spiked connecting scaffold for resurfacing THA endoprostheses: a pilot study. *J Clinic Med.* 2021;10(13):2937. doi: 10.3390/jcm10132937
85. Lu J, Gao Y, Cao C, *et al.* 3D bioprinted scaffolds for osteochondral regeneration: advancements and applications. *Mater Today Bio.* 2025;32:101834. doi: 10.1016/j.mtbio.2025.101834
86. Gao D, Li R, Pan J, *et al.* 3D bioprinting bone/cartilage organoids: construction, applications, and challenges. *J Orthop Translat.* 2025;55:75-93. doi: 10.1016/j.jot.2025.08.008
87. Wang J, Chen X, Li R, *et al.* Standardization and consensus in the development and application of bone organoids. Review. *Theranostics.* 2025;15(2):682-706. doi: 10.7150/thno.105840
88. Ohman-Magi C, Holub O, Wu D, Hall RM, Persson C. Density and mechanical properties of vertebral trabecular bone: a review. *JOR Spine.* Dec 2021;4(4):e1176. doi: 10.1002/jsp2.1176
89. Inzana JA, Olvera D, Fuller SM, *et al.* 3D printing of composite calcium phosphate and collagen scaffolds for bone regeneration. *Biomaterials.* 2014;35(13):4026-4034. doi: 10.1016/j.biomaterials.2014.01.064
90. Bendtsen ST, Quinnell SP, Wei M. Development of a novel alginate-polyvinyl alcohol-hydroxyapatite hydrogel for 3D bioprinting bone tissue engineered scaffolds. *J Biomed Mater Res A.* 2017;105(5):1457-1468. doi: 10.1002/jbm.a.36036
91. Monavari M, Medhekar R, Nawaz Q, *et al.* A 3D printed bone tissue engineering scaffold composed of alginate dialdehyde-gelatin reinforced by lysozyme loaded cerium doped mesoporous silica-calcia nanoparticles. *Macromol Biosci.* 2022;22(9):e2200113. doi: 10.1002/mabi.202200113
92. Ojansivu M, Rashad A, Ahlinder A, *et al.* Wood-based nanocellulose and bioactive glass modified gelatin-alginate bioinks for 3D bioprinting of bone cells. *Biofabrication.* 2019;11(3):035010. doi: 10.1088/1758-5090/ab0692
93. Wang LL, Highley CB, Yeh YC, Galarraga JH, Uman S, Burdick JA. Three-dimensional extrusion bioprinting of single- and double-network hydrogels containing dynamic covalent crosslinks. *J Biomed Mater Res A.* 2018;106(4):865-875. doi: 10.1002/jbm.a.36323
94. Zhang X, Yan Z, Guan G, *et al.* Polyethylene glycol diacrylate scaffold filled with cell-laden methacrylamide gelatin/alginate hydrogels used for cartilage repair. *J Biomater Appl.* 2022;36(6):1019-1032. doi: 10.1177/08853282211044853
95. Hsieh CT, Hsu SH. Double-network polyurethane-gelatin hydrogel with tunable modulus for high-resolution 3D bioprinting. *ACS Appl Mater Interfaces.* 2019;11(36):32746-32757. doi: 10.1021/acsami.9b10784
96. Lee J, Hong J, Kim W, Kim GH. Bone-derived dECM/alginate bioink for fabricating a 3D cell-laden mesh structure for bone tissue engineering. *Carbohydr Polym.* 2020;250:116914. doi: 10.1016/j.carbpol.2020.116914
97. Chen Z, Zhang H, Huang J, *et al.* DNA-encoded dynamic hydrogels for 3D bioprinted cartilage organoids. *Mater Today Bio.* 2025;31:101509. doi: 10.1016/j.mtbio.2025.101509
98. Leite AJ, Sarker B, Zehnder T, Silva R, Mano JF, Boccaccini AR. Bioplotting of a bioactive alginate dialdehyde-gelatin composite hydrogel containing bioactive glass nanoparticles. *Biofabrication.* 2016;8(3):035005. doi: 10.1088/1758-5090/8/3/035005
99. Korkeamaki JT, Rashad A, Ojansivu M, *et al.* Systematic development and bioprinting of novel nanostructured multi-material bioinks for bone tissue engineering. *Biofabrication.* 2025;17(2):025005. doi: 10.1088/1758-5090/ada63b
100. Liu B, Li J, Lei X, *et al.* 3D-bioprinted functional and biomimetic hydrogel scaffolds incorporated with nanosilicates to promote bone healing in rat calvarial defect model. *Mater Sci Eng C Mater Biol Appl.* 2020;112:110905. doi: 10.1016/j.msec.2020.110905
101. Mathur V, Agarwal P, Kasturi M, Srinivasan V, Seetharam RN, Vasanthan KS. Innovative bioinks for 3D bioprinting: exploring technological potential and regulatory challenges. *J Tissue Eng.* 2025;16:20417314241308022. doi: 10.1177/20417314241308022
102. Bastos AR, da Silva LP, Maia FR, *et al.* Hydroxyapatite/alginate/gellan gum inks with osteoconduction and osteogenic potential for bioprinting bone tissue analogues. *Int J Biol Macromol.* 2024;271(Pt 2):132611. doi: 10.1016/j.ijbiomac.2024.132611
103. Yang J, Chen Z, Gao C, *et al.* A mechanical-assisted post-bioprinting strategy for challenging bone defects repair. *Nat Commun.* 2024;15(1):3565. doi: 10.1038/s41467-024-48023-8
104. Ebrahimi Sadrabadi A, Baei P, Hosseini S, Baghaban Eslaminejad M. Decellularized extracellular matrix as a potent natural biomaterial for regenerative medicine. *Adv Exp Med Biol.* 2021;(1341):27-43. doi: 10.1007/5584\_2020\_504
105. Baroncelli M, Van Der Eerden BC, Chatterji S, *et al.* Human osteoblast-derived extracellular matrix with high homology to bone proteome is osteopromotive. *Tissue Eng Part A.* 2018;24(17-18):1377-1389.

- doi: 10.1089/ten.TEA.2017.0448
106. Jones L, Thomsen JS, Mosekilde L, Bosch C, Melsen B. Biomechanical evaluation of rat skull defects, 1, 3, and 6 months after implantation with osteopromotive substances. *J Craniomaxillofac Surg.* 2007;35(8):350-357. doi: 10.1016/j.jcms.2007.06.004
107. Biehl A, Gracioso Martins AM, Davis ZG, et al. Towards a standardized multi-tissue decellularization protocol for the derivation of extracellular matrix materials. *Biomater Sci.* 2023;11(2):641-654. doi: 10.1039/d2bm01012g
108. Ramos-Rodriguez DH, Leach JK. Decellularized cell-secreted extracellular matrices as biomaterials for tissue engineering. *Small Sci.* 2025;5(2):2400335. doi: 10.1002/smssc.202400335
109. Cao B, Zhang K, Zuo R, et al. 3D-bioprinted functional scaffold based on synergistic induction of i-PRF and laponite exerts efficient and personalized bone regeneration via miRNA-mediated TGF-beta/Smads signaling. *Int J Surg.* 2025;111(5):3193-3211. doi: 10.1097/JS9.0000000000002312
110. Deng Y, Yang W-Z, Shi D, et al. Bioinspired and osteopromotive polydopamine nanoparticle-incorporated fibrous membranes for robust bone regeneration. *NPG Asia Mater.* 2019;11(1):39. doi: 10.1038/s41427-019-0139-5
111. Grasmik V, Breisch M, Loza K, et al. Synthesis and biological characterization of alloyed silver-platinum nanoparticles: from compact core-shell nanoparticles to hollow nanoalloys. *RSC Adv.* 2018;8(67):38582-38590. doi: 10.1039/c8ra06461j
112. Wolff N, Bialas N, Loza K, et al. Increased cytotoxicity of bimetallic ultrasmall silver-platinum nanoparticles (2 nm) on cells and bacteria in comparison to silver nanoparticles of the same size. *Materials (Basel).* 2024;17(15):3702. doi: 10.3390/ma17153702
113. Seo JJ, Mandakhbayar N, Kang MS, et al. Antibacterial, proangiogenic, and osteopromotive nanoglass paste coordinates regenerative process following bacterial infection in hard tissue. *Biomaterials.* 2021;268:120593. doi: 10.1016/j.biomaterials.2020.120593
114. Sadeghianmaryan A, Naghieh S, Yazdanpanah Z, et al. Fabrication of chitosan/alginate/hydroxyapatite hybrid scaffolds using 3D printing and impregnating techniques for potential cartilage regeneration. *Int J Biol Macromol.* 2022;204:62-75. doi: 10.1016/j.ijbiomac.2022.01.201
115. Seok JM, Kim MJ, Park JH, et al. A bioactive microparticle-loaded osteogenically enhanced bioprinted scaffold that permits sustained release of BMP-2. *Mater Today Bio.* 2023;21:100685. doi: 10.1016/j.mtbio.2023.100685
116. Osidak EO, Kozhukhov VI, Osidak MS, Domogatsky SP. Collagen as bioink for bioprinting: a comprehensive review. *Int J Bioprint.* 2020;6(3):270. doi: 10.18063/ijb.v6i3.270
117. Hogan KJ, Oztatli H, Perez MR, et al. Development of photoreactive demineralized bone matrix 3D printing colloidal inks for bone tissue engineering. *Regen Biomater.* 2023;10:rbad090. doi: 10.1093/rb/rbad090
118. Im S, Choe G, Seok JM, et al. An osteogenic bioink composed of alginate, cellulose nanofibrils, and polydopamine nanoparticles for 3D bioprinting and bone tissue engineering. *Int J Biol Macromol.* 2022;205:520-529. doi: 10.1016/j.ijbiomac.2022.02.012
119. Ghosh S, Webster TJ. Metallic nanoscaffolds as osteogenic promoters: advances, challenges and scope. *Metals.* 2021;11(9):1356. doi: 10.3390/met11091356
120. Palivela BC, Bandari SD, Mamilla RS. Extrusion-based 3D printing of bioactive glass scaffolds-process parameters and mechanical properties: a review. *Bioprinting.* 2022;27:e00219.
121. Badhe RV, Chatterjee A, Bijukumar D, Mathew MT. Current advancements in bio-ink technology for cartilage and bone tissue engineering. *Bone.* 2023;171:116746. doi: 10.1016/j.bone.2023.116746
122. Genova T, Roato I, Carossa M, Motta C, Cavagnetto D, Mussano F. Advances on bone substitutes through 3D bioprinting. *Int J Mol Sci.* 2020;21(19):7012. doi: 10.3390/ijms21197012
123. Bahraminasab M. Challenges on optimization of 3D-printed bone scaffolds. *Biomed Eng Online.* 2020;19(1):69. doi: 10.1186/s12938-020-00810-2
124. Midha S, Dalela M, Sybil D, Patra P, Mohanty S. Advances in three-dimensional bioprinting of bone: progress and challenges. *J Tissue Eng Regen Med.* 2019;13(6):925-945. doi: 10.1002/term.2847